ARTICLE

Lipid droplet screen in human hepatocytes identifies TRRAP as a regulator of cellular triglyceride metabolism

Deepti Abbey[1,2] | Donna Conlon[1,2] | Christopher Rainville[3] | Susannah Elwyn[1,2] |
Katherine Quiroz-Figueroa[1,2] | Jeffrey Billheimer[2] | David C. Schultz[3] |
Nicholas J. Hand[1] | Sara Cherry[4] | Daniel J. Rader[1,2,5]

[1]Department of Genetics, University of Pennsylvania, Philadelphia, Pennsylvania, USA

[2]Division of Translational Medicine and Human Genetics, Department of Medicine, University of Pennsylvania, Philadelphia, Pennsylvania, USA

[3]High Throughput Screening Core, Department of Microbiology, University of Pennsylvania, Philadelphia, Pennsylvania, USA

[4]Department of Microbiology, University of Pennsylvania, Philadelphia, Pennsylvania, USA

[5]Cardiovascular Institute, University of Pennsylvania, Philadelphia, Pennsylvania, USA

Correspondence
Daniel J. Rader, Department of Genetics, University of Pennsylvania, Philadelphia, PA, USA.
Email: rader@pennmedicine.upenn.edu

Abstract

Hepatocytes store triglycerides (TGs) in the form of lipid droplets (LDs), which are increased in hepatosteatosis. The regulation of hepatic LDs is poorly understood and new therapies to reduce hepatosteatosis are needed. We performed a siRNA kinase and phosphatase screen in HuH-7 cells using high-content automated imaging of LDs. Changes in accumulated lipids were quantified with developed pipeline that measures intensity, area, and number of LDs. Selected "hits," which reduced lipid accumulation, were further validated with other lipid and expression assays. Among several siRNAs that resulted in significantly reduced LDs, one was targeted to the nuclear adapter protein, transformation/transcription domain-associated protein (TRRAP). Knockdown of TRRAP reduced triglyceride accumulation in HuH-7 hepatocytes, in part by reducing C/EBPα-mediated de novo synthesis of TGs. These findings implicate TRRAP as a novel regulator of hepatic TG metabolism and nominate it as a potential drug target for hepatosteatosis.

Study Highlights

WHAT IS THE CURRENT KNOWLEDGE ON THE TOPIC?
Non-alcoholic fatty liver disease is a major public health issue that is not well-understood and has limited therapeutic options.
WHAT QUESTION DID THIS STUDY ADDRESS?
The purpose of the study was to identify novel candidates involved with lipid metabolism, and understand their influence in hepatosteatosis.
WHAT DOES THIS STUDY ADD TO OUR KNOWLEDGE?
The study proposes a robust high-throughput approach for identifying potential candidates involved with lipid metabolism. Transformation/transcription domain-associated protein, a nuclear adapter protein, was identified that regulates hepatic triglyceride metabolism and serves as a potential target for hepatosteatosis. The approach can be extended to other model systems to identify novel genes and pathways by phenotypic screening approach to search for unmet need for therapies.

INTRODUCTION

Hepatic lipid droplets (LDs) mainly consist of triglycerides (TGs)[1–3] and are regulated by a dynamic process of lipid synthesis, TG hydrolysis, fatty acid ß-oxidation, and TG secretion.[4,5] Accumulation of LDs in hepatocytes is the characteristic feature of non-alcoholic fatty liver disease (NAFLD), which is often associated with obesity, type 2 diabetes, and dyslipidemia, and can progress to non-alcoholic steatohepatitis and hepatic fibrosis.[6,7] Some of the pathways and key proteins responsible for hepatocyte LD formation, growth, and interaction with different organelles have been elucidated.[3] However, there is still a lack of understanding about the processes that influence LD accumulation in the liver and there is a relative lack of validated therapeutic targets for the treatment of NAFLD.[8,9]

In recent years, the advent of high throughput RNAi screens has enabled the study of cell biological processes in an unbiased manner.[10] Furthermore, high-content screening (HCS) has made it possible to use imaging in high-throughput screens.[11] A few reports of image-based RNAi screens have been performed to dissect the biology of LDs.[12,13] However, these studies used BODIPY for LD imaging, which is confounded by high background staining and rapid signal photo-bleaching. Further, LD quantification by colorimetric biochemical assay lacks precision and sensitivity for discrimination between variable sized LDs and cell debris.[14] To facilitate the search for new molecules and potential therapeutic targets involved with hepatocyte TG metabolism and LD formation, we established a high throughput screening platform for the quantification of LD accumulation in human HuH-7 cells using a high-content cell-based fluorescent imaging assay. A focused high-throughput HCS against the kinome and phosphatome was performed using this platform. We identified several novel candidates regulating LDs, including transformation/transcription domain-associated protein (TRRAP), which we demonstrate is involved in the regulation of TG synthesis and accumulation in hepatocytes.

MATERIALS AND METHODS

Cells

HuH-7 cells were from the JCRB cell bank and maintained in DMEM with 10% fetal bovine serum (FBS) and 1% antibiotics. Cell line was checked for mycoplasma and other contaminants.

High-throughput siRNA screen

The Ambion Silencer Select (Life Technologies) siRNA library was arrayed in 384-well plates with 3 siRNAs against a single gene target pooled in one well. Assay ready plates (384-well) were prepared by spotting 1 µl of 1.5 µM siRNA from a stock plate, heat sealed, and stored at −80°C until use. Each assay plate contains siRNAs to 352 independent gene targets. Prior to use, assay plates were thawed at room temperature and 1 µl of 1.5 µM control siRNAs were manually added to columns 23 and 24. For negative controls, cells were transfected with 30 nM siRNA against GAPDH, Luciferase, GFP, and sequences that do not target a human cellular gene, respectively. As a positive control for functional transfection, cells were transfected with 30 nM siDeath (Qiagen). Lipofectamine RNAiMAX (0.1 µl/well) was diluted in OptiMEM (Invitrogen) and equilibrated for 30 min at room temperature prior to dispensing 10 µl to siRNA containing assay ready plates using a Multidrop Combi Reagent Dispenser (Thermo Scientific). The siRNA lipid mixture was incubated at room temperature for 30 min. Then, 40 µl of HuH-7 cells (500/well) in antibiotic free DMEM with 10% FBS was dispensed to assay plates using a Multidrop combi. Assay plates were incubated for 3 days at 37°C, 5% CO_2, and 20% O_2 in a humidified chamber. Growth medium removed and cells were refed with 40 µl DMEM with 1.5% bovine serum albumin (BSA). Plates were incubated for an additional 24 h at 37°C, 5% CO_2, and 20% O_2. Cells were fixed with 4% formaldehyde and then stained with a 1:1000 dilution of LipidTox (ThermoFisher) and nuclei were counterstained with 4 µg/ml Hoechst dye. LDs and nuclei were imaged at ×10 on an automated ImageXpress Micro (Molecular Devices), 4 sites per well. The number of nuclei, LDs, LD intensity, and LD area were quantified using a Granularity application module in Metaxpress version 5.3.05, (Molecular Devices). Nuclei counts, LD count, LD intensity, and LD area were normalized to aggregated negative control wells and expressed as percentage of control (POC = observed/$NegC_{avg}$) and z-score (Z-score = observed-$NegC_{avg}$/$NegC_{stdev}$) in Spotfire (PerkinElmer). Candidate hits were defined by a z-score less than or equal to −1.5. Captured images were further scored to validate the reported change in LD intensity, number, area, and localization of LDs.

LipidTOX staining

HuH-7 cells were washed with phosphate-buffered saline (PBS) and incubated with LipidTOX (1:1000) and DAPI for

30 min in the dark at room temperature. After 30 min, staining solution was replaced with PBS and plates were stored in the dark at 4°C until imaging.

Triglyceride measurement

For detection of TGs by colorimetric enzymatic assay, HuH-7 cells were washed with PBS and incubated with 3:2 Hexane: Isopropanol for 2 h. Extracted lipid was dried under N_2 and reconstituted in 500 µl of 15% Triton X-100 in chloroform. Later, it was dried under N_2 and reconstituted in 30 µl of water. Then, 10 µl of extracted lipid was used for colorimetric TGs measurement by enzymatic assay (ThermoFisher) using commercial lipid standard.

For detection of newly synthesized TGs, HuH-7 cells were incubated with 10 µCi/ml of 1,2,3-[³H] Glycerol (American Radiolabeled Chemicals) with 0.2 mM oleic acid (OA) for 4 h. Lipid was extracted from cells using 3:2 hexane:isopropanol according to the method of Bligh and Dyer[15] and media using 2:1 chloroform:methanol using the Folch method[16] and was dried under N_2 gas. It was then resuspended in hexane, spotted, and separated on silica 60 TLC plates and visualized using iodine. Total protein was recovered by solubilizing the remaining cells in 0.1 N NaOH and measured using bicinchoninic acid (BCA) assay (Pierce, Thermo Fisher Scientific). Measured lipid counts were then normalized to the total cell protein from respective wells.

De novo lipogenesis

For de novo lipogenesis, HuH-7 cells were labeled with 1 µCi/ml of ¹⁴C-Acetate for 1 h. Lipid was extracted as described above and separated on TLC. The mobile phase used for lipid separation consists of hexane:diethyl ether:acetic acid (170:30:1) and visualized using iodine. The plasma lipids (PLs), fatty acid (FA), TGs, and cholesterol ester spots were scraped, and the counts in each spot were measured using a beta counter (Beckman Coulter). Counts were measured and normalized to protein from respective wells as measured by BCA.

ApoB100 measurement

At 72 h post-transfection, the media of HuH-7 cells was replaced with serum free and methionine- and cysteine-free DMEM with 1.5% BSA for 2 h and then labeled for 2 h with 200 µCi of [³⁵S] methionine/cysteine labeling mix (PerkinElmer Life Sciences) in the same media. At the end of the 2-h label, the media was collected and cells were lysed. Immunoprecipitation of proteins from each sample was carried out by incubating media and cell lysates with antibodies against apoB (Calbiochem) or albumin (Sigma) and Protein A-agarose at 4°C for an additional 16 h. The beads were washed with NET buffer, and proteins were released with sample buffer (0.125 M Tris-HCl [pH 6.8], 4% sodium dodecyl sulfate [SDS], 20% glycerol, and 10% β-mercaptoethanol) by boiling for 5 min. Samples were resolved by gel electrophoresis followed by autoradiography to detect total amount of newly synthesized apoB100 and albumin, which was then normalized to the total [³⁵S] trichloroacetic acid precipitable counts in each sample.

Fatty acid oxidation

HuH-7 cells were incubated with labeled media consisting of DMEM with 1.5% BSA, 0.1 mM OA, and ¹⁴C OA (1 µCi/ml) for 2 h for FA oxidation measurement, as described previously.[17] Briefly, cells were chased with DMEM + 1.5% BSA for 4 h, after which the media were collected for FA oxidation measurement. At the end of the labeling or chase period, the media were transferred to sealed Erlenmeyer flasks. Lipid oxidation was stopped with the addition of 200 µl of 70% perchloric acid to the bottom of the flask, driving the bicarbonate into CO_2. The ¹⁴CO_2 was captured on a piece of KOH-soaked filter paper. After incubating the filter paper in the flask for 1 h at room temperature, the filter paper was analyzed for ¹⁴C activity by liquid scintillation counting of ¹⁴CO_2. The media remaining in the flask were collected and a fraction counted for ¹⁴C as a measure of ASM production. After the labeled and chase media were removed at the end of the experiment, lipid was extracted and ¹⁴C counts were measured, as described above, and normalized to the protein from respective wells as measured by BCA.

Quantitative real-time polymerase chain reaction

RNA was isolated from cells using Zymo kits. The cDNA was prepared from 1 µg RNA using random hexamers and oligodT (1:1) following manufacturer's instructions (Applied Biosystems). For quantitative polymerase chain reaction, Taqman probes were used for respective genes with 10 ng cDNA run in duplicates. GAPDH was used as reference gene.

Western blotting

HuH-7 cells were lysed using RIPA buffer and lysate was used for protein estimation following BCA assay. Then, 20 µg of lysate was separated on 3–8% tris-acetate and 4–12%

SDS-acrylamide gels and transferred on polyvinylidene difluoride membranes. Membranes were incubated with primary antibodies (Abs) overnight and then with species-specific HRP-conjugated secondary Abs. Protein bands were visualized using SuperSignal West Pico Chemiluminescent Substrate (Thermo Fisher Scientific). TRRAP (CST), C/EBPA (CST), LXRA (Active Motif), FASN (CST), and Beta-Actin (SantaCruz Biotechnology) were used.

Enzyme-linked immunosorbent assay

Apolipoprotein C3 (APOC3) in medium was measured using commercial enzyme-linked immunosorbent assay (ELISA) kit (Thermo Fisher / RayBiotech).

Statistical analysis

The primary screen was performed in triplicate, and POC and z scores relative to negative control wells were calculated based on SD across each plate. In additional follow-up studies, all quantitative data represent mean ± SEM. Student's t-test with Welch's correction was used to determine significance following GraphPad Prism version 8 for Mac.

RESULTS

Kinome-wide RNAi screen identified regulators of hepatic triglyceride metabolism

To establish a platform for LD screening suitable for large-scale high-content automated imaging in HuH-7 cells, we optimized different parameters required for a quantifiable and reproducible assay for LDs post-siRNA transfections. HuH-7 cells were grown in a clear bottom 384-well microtiter plates (seeded at ~ 500 cells/well) and transfected with siRNA at a final concentration of 20 nM. After 72 h, medium was replaced with serum-free medium and 24 h later cells were fixed, stained with LipidTOX,[14,18] and imaged by automated image analysis (Figure 1a). Transfections were efficient as indicated by ~ 99% dead cells in siDeath (transfection control) transfected wells in replicate experiments (Figure 1b). OA treatment was used to demonstrate induction of LDs, and cells were transfected with siRNA against DGAT2, a key player involved in TG synthesis,[19] as a positive control for reduction in LDs (Figure 1b). Quantification of number, area, and intensity of LDs was performed.[12,20,21] As expected, OA treatment increased number, size, and density of LDs; however, even HuH-7 cells not treated with OA had substantial LDs and exhibited less variability than OA-treated cells, consistent with a previous observation made in HepaRG cells.[22]

Therefore, OA induction was not used for the primary high-content screen. For internal imaging controls, transfection with siRNA against GFP and luciferase was used, spotted randomly in the plate, as shown in the heat map for total integrated intensity of LDs (Figure 1c and Figure S1a,b). For stringent quantitative representation of the lipid phenotype and to rule out the possible cytotoxic effect, only wells that had greater than 60% of live cells/well were included in the analysis.

We screened a library of 1056 human kinases and phosphatases, based on their known significant contribution in the druggable genome.[23] Our high-content screening assay quantitated: (i) intensity of LDs, (ii) number of LDs, and (iii) area of LDs per cell. Screening was performed in triplicate with 3 siRNAs per a gene target in a single well of 384-well plates. We observed a good correlation between the replicate plates (Figure 1d) with an overall Z'-factor of 0.64 for the screen (Figure 1e). DGAT2 was used as a positive control in the screen, and siRNAs to DGAT2 showed fivefold reduced LipidTOX intensity as well as reduction in number of LDs (Figure 1f,g). "Candidate hits" were defined based upon the decrease in intensity of LDs compared with the negative-control transfected wells. The top 2% of genes (z score cut-off ≤ -1.5; total 22 candidates; Figure S1c and Table S1) that decreased the intensity of LDs were selected for further analysis. Glucose-6-phosphatase, catalytic 3 was included as an internal imaging control, knockdown of which showed no significant effect on LDs intensity and LDs number (z score: 1.15; Figure S2, Table S1).

Seven of the 22 candidate hits were considered for follow-up secondary experiments based upon several biological considerations, including no known prior relationship to TG metabolism or LD formation (Figure 1f and Table S2). To validate these gene targets, we performed independent siRNA transfections in bigger wells (96- and 6-well plates) of HuH-7 cells and analyzed several parameters including: (i) degree of mRNA knockdown, (ii) LD accumulation by LipidTOX staining, (iii) colorimetric TG biochemical assay, (iv) gene expression of selected candidate genes, and (v) APOC3 protein mass in media (Table S2). Knockdown of all seven follow-up candidates showed decrease in LipidTOX stained LD quantification and TG accumulation by colorimetric assay (Figure S2a and Table S2). Gene expression profiling showed a significant decrease in transcripts of selected candidate hits on siRNA knockdown, except for FLT1, which was not significantly detectable in HuH7 cells (Figure S2b). Knockdown of candidate hits either showed decreased expression of genes involved with TG synthesis, as DGAT2, or increased expression of genes involved with lipid hydrolysis, such as LIPC (Figure S2b). Three candidates (TRRAP, DUT, and ALDH18A1) showed a significant decrease in TGs measured by colorimetric assay, as well as in secreted APOC3 in the media (Figure S2a and S2c). After
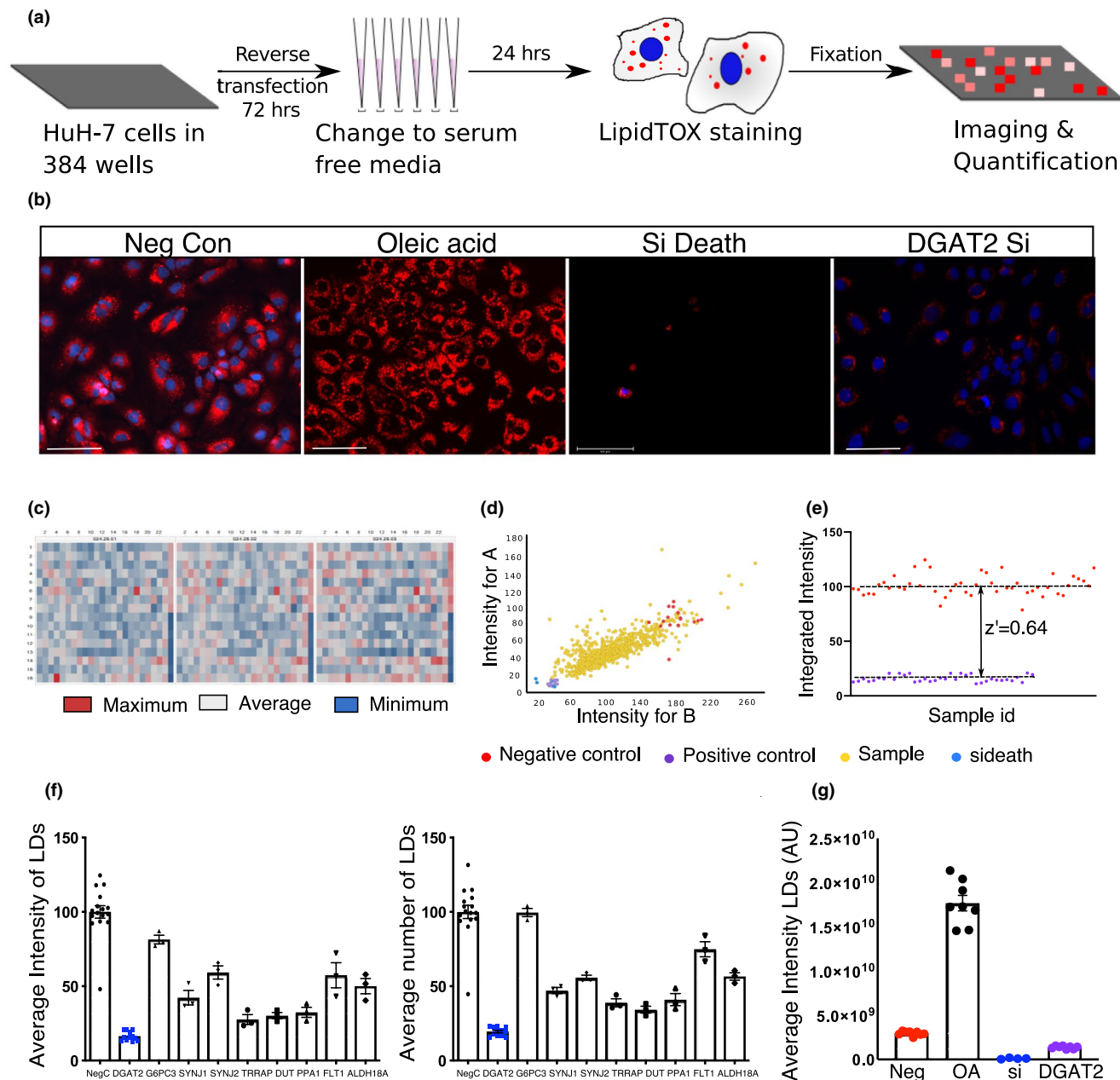
FIGURE 1 High-content genome-wide kinome screen identified genes that reduced lipid droplets (LDs) in HuH-7 cells. (**a**) Schematic showing strategy used to screen for genes affecting triglyceride (TG) accumulation. (**b**) Representative images showing LipidTOX stained negative control, oleic acid (OA)-induced, siDeath, and DGAT2 transfected HuH-7 cells, where OA and DGAT2 were used as positive controls. (**c**) Heatmap showing integrated intensity among replicate plates (red = maximum, white = average, and blue = minimum). (**d**) Dotplot showing correlations between LD intensity on knockdown of kinases/phosphatases for replicate plates A and B. (**e**) The Z' for LD intensity assay. (**f**) Knockdown of selected candidate genes decreases LD intensity and LD number when compared to negative control wells. (**g**) LipidTOX quantification of DGAT2 transfected and OA-induced HuH-7 cells (error bar represents SEM for 3 replicates). Scale bar = 125 μm

lipid-loading with OA, knockdown of TRRAP and DUT still decreased secreted APOC3 (Figure S2c). Mutations in ALDH18A1 have been previously associated with a defective LD phenotype,[24] and there has been a report of a possible interaction of DUT with PPARα.[25] Thus, we elected to further pursue TRRAP as a novel potential regulator of hepatocyte LD formation.

Knockdown of TRRAP reduced cellular TG by affecting de novo lipid synthesis and not TG secretion

TRRAP is an adapter protein that has been identified as a member of various histone acetyltransferase activity (HAT) multiprotein complexes and is involved in transcriptional

regulation.[26] TRRAP has never been implicated in TG metabolism. We performed validation of TRRAP knockdown in 6-well plates. Efficient knockdown of ~ 80% in TRRAP was observed with the pool of siRNAs, as quantified by Western blotting. TRRAP knockdown decreased LDs by ~ 30% as compared with negative control wells (Figure 2a and Table S3), and decreased TG mass by ~ 35% (Figure 2b). Thus, TRRAP knockdown reproducibly and robustly reduces LDs and TGs
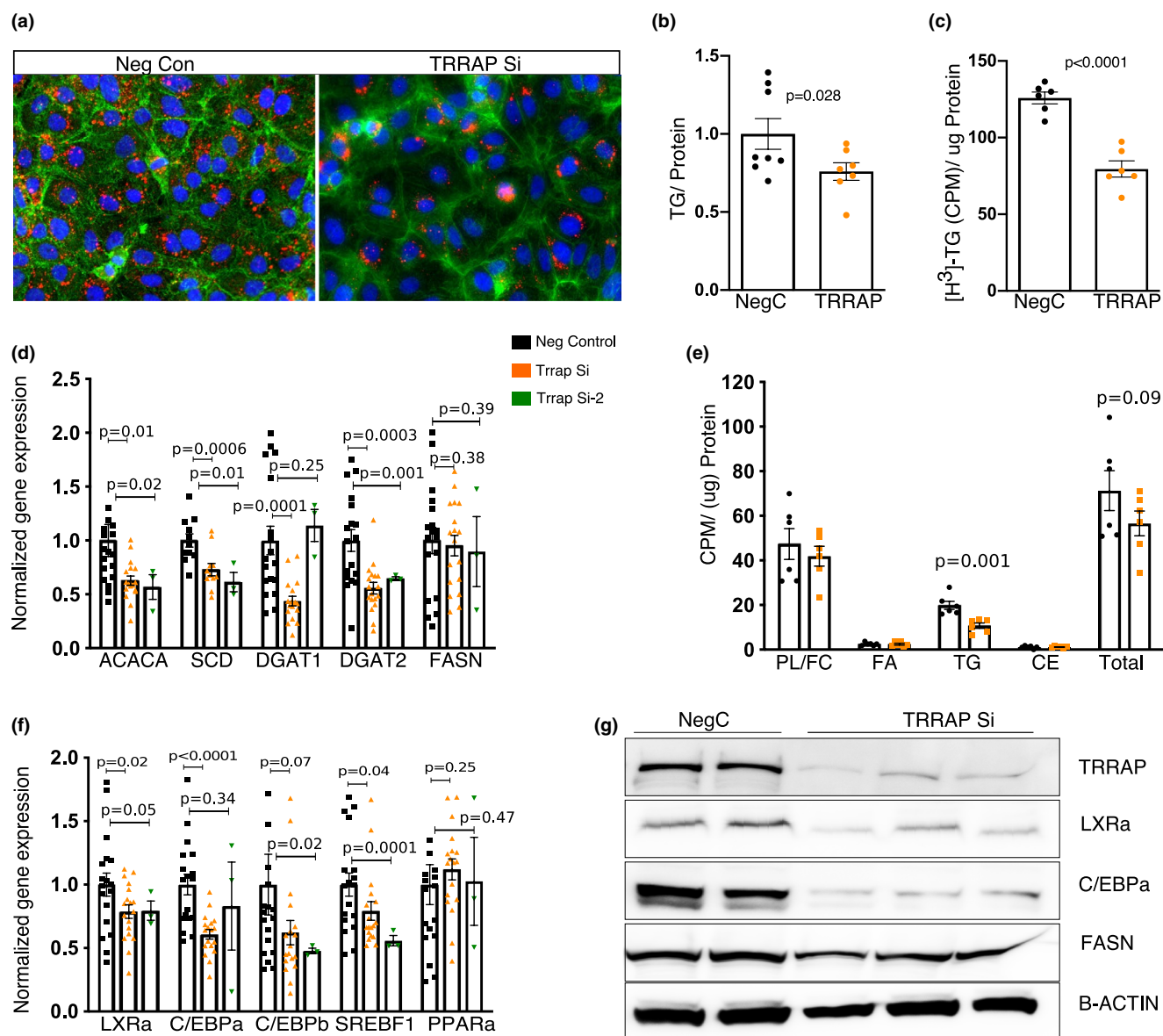

FIGURE 2 Transformation/transcription domain-associated protein (TRRAP) knockdown reduces triglycerides (TGs) accumulation in HuH-7 cells by reducing de novo lipogenesis (DNL). (**a**) Representative images showed LipidTOX staining in HuH-7 cells, when transfected with negative control and TRRAP siRNA. (**b, c**) Confirmation of the phenotype with colorimetric TG assay and radiolabel [^{3}H]-1,2,3-glycerol assay showed reduced TG accumulation in HuH-7 cells on TRRAP knockdown. Cells were lysed after 72 h post-transfection, and lipid was extracted for colorimetric assessment. HuH-7 cells were labeled with [^{3}H]-Glycerol with 0.2 mM oleic acid (OA) for 4 h, and lipids were extracted for measuring counts. (**d**) Quantitative polymerase chain reaction (q-PCR) analysis showed a decrease in the expression of genes involved with TG synthesis (*DGAT1, DGAT2, SCD1, FASN*, and *ACACA*) on knockdown of TRRAP in HuH-7 cells. (**e**) For measuring de novo lipogenesis, HuH-7 cells were labeled with ^{14}C-Acetate (1 μCi/ml) for 1 h; lipid was extracted and separated on TLC. Counts were measured and normalized to total protein as measured by bicinchoninic acid (BCA). (**f**) q-PCR analysis showed decrease in the expression of transcription factors involved with lipid metabolism such as *C/EBPα, C/EBPB, LXRα*, and *SREBF1* but not in *PPARα* in TRRAP siRNA compared with negative control transfected HuH-7 cells. (**g**) Western blots showed decreased protein expression of TRRAP, LXRA, C/EBPα, and FASN on TRRAP knockdown in HuH-7 cells. Beta-actin was used as loading control. q-PCR results were normalized to GAPDH. For densitometric quantification, labeling experiments and q-PCR, control values were defined as 1 and changes in TRRAP transfected cells expressed as relative amounts compared with controls. All data represent the mean ±SEM. The *p* values were calculated with Welch's test

in HuH-7 cells. No significant reduction in either LD intensity or LD number was observed upon TRRAP knockdown in the presence of exogenous OA treatment (Figure S3 and Table S4).

TRRAP knockdown could reduce LDs and TGs by decreasing lipid synthesis, increasing lipolysis, increasing FA ß-oxidation, or increasing secretion of TGs. To assess newly synthesized TGs, we used labeling with 1,2,3-[^{3}H]-glycerol. A significant reduction in incorporation of [^{3}H]-glycerol into cellular TGs by 38% was observed in TRRAP knockdown cells when compared with negative control transfected cells (Figure 2c). TRRAP knockdown resulted in decreased expression of de novo lipogenesis (DNL) genes, including *ACACA, DGAT1, DGAT2, FASN*, and *SCD1* (Figure 2d) and also reduced the protein abundance of FASN (Figure 2g). To stringently assess the effect of knockdown, we used a completely different pool of siRNAs against TRRAP and observed a similar decrease in the expression of DNL genes (Figure 2d). We performed a de novo lipid synthesis assay using ^{14}C-acetate, and upon TRRAP knockdown the incorporation of newly synthesized FAs into TGs was decreased by ~ 46% (Figure 2e).

Knockdown of TRRAP reduced expression of LXRα and C/EBPα and expression and secretion of APOC3

We analyzed the mRNA abundance of major transcription factors involved with lipid metabolism. Knockdown of TRRAP significantly decreased the gene expression of *LXRα, LXRβ, C/EBPα, C/EBPβ*, and *SREBF1*, but not *PPARα* (Figure 2f). Consistent with this observation, we noted decreased protein for LXRα (−41%) and C/EBPα (−63%; Figure 2g). A similar observation was made with a different pool of siRNAs used against TRRAP (Figure 2d,f). Thus, TRRAP may modulate hepatic TG metabolism through its effects on LXRα and C/EBPα expression.

We did not observe significant changes in the secretion of newly synthesized TGs after labeling with ^{3}H-glycerol in TRRAP knockdown cells (Figure 3a). Similarly, no difference was observed in the secretion of newly synthesized ApoB100 in TRRAP knockdown cells when compared with negative control (Figure 3b–d). In addition, no differences in the gene expression for genes involved with transport (*MTTP*) and FA oxidation (*ACOX1* and *CPT1A*) were observed on TRRAP knockdown, when analyzed with two different pools of siRNAs (Figure 4a). There was no significant difference observed in the amount of ^{14}CO$_2$ released and ^{14}C acid-soluble metabolites (ASMs) produced during 2-h of labeling with ^{14}C-OA treatment in TRRAP knockdown HuH-7 cells (Figure 4b). Thus, TRRAP knockdown does not appear to affect TG secretion or FA oxidation.

APOC3 is an important regulator of triglyceride-rich lipoprotein metabolism[27] and a drug target for hypertriglyceridemia and coronary heart disease[28]; APOC3 has also been implicated in NAFLD,[29,30] suggesting that secreted APOC3 might be useful as a biomarker. We observed a consistent
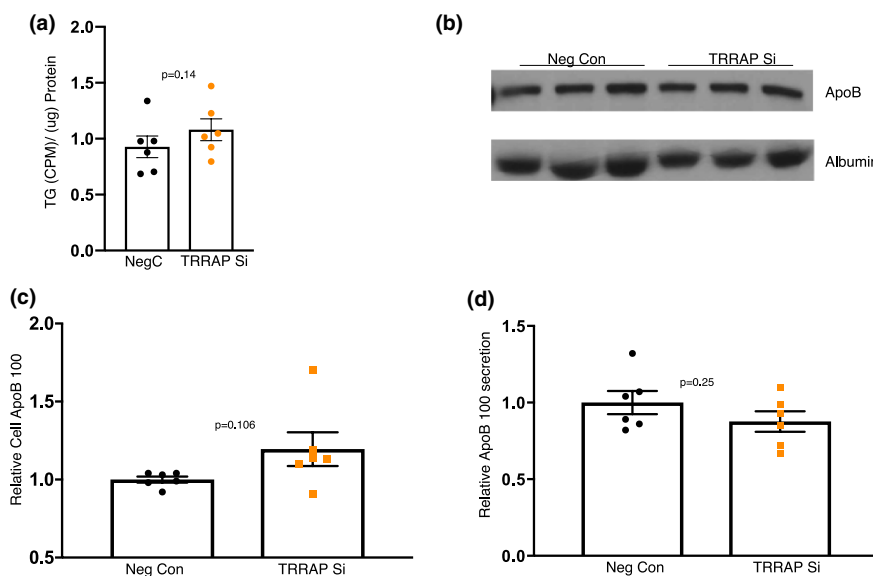

FIGURE 3 Knockdown of transformation/transcription domain-associated protein (TRRAP) does not affect secretion of TGs and APOB-100. (**a**) Triglycerides (TGs) were measured in the medium after labeling HuH-7 cells with [^{3}H]-Glycerol with 0.2 mM oleic acid (OA) for 4 h. No difference was observed on TRRAP knockdown when compared with negative control transfected HuH-7 cells. (**b–d**) Negative control and TRRAP siRNA transfected HuH-7 cells were radiolabeled with 200 μCi/ml of ^{35}S-methionine/cysteine for 2 h after serum starvation of 2 h, followed by immunoprecipitation of ApoB or albumin from conditioned media and cell lysate, sodium dodecyl sulfate (SDS)-polyacrylamide gel electrophoresis and autoradiography. Albumin was used for normalization. ApoB measurements were normalized to radioactive counts in trichloroacetic acid precipitated proteins from each cell lysate. The *p* values were calculated with Welch's test
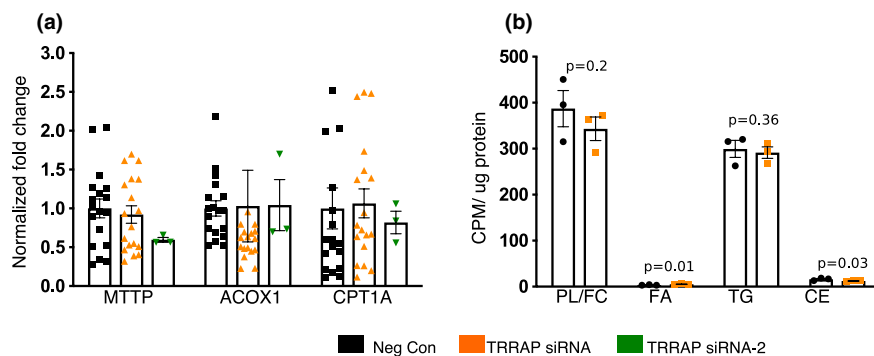
FIGURE 4 Transformation/transcription domain-associated protein (TRRAP) knockdown has no effect on very low-density lipoprotein-triglyceride (VLDL-TG) transport and fatty acid-oxidation. (**a**) Quantitative polymerase chain reaction (q-PCR) analysis showed no change in the gene expression of *MTTP*, *ACOX1*, and *CPT1A* genes, involved with fatty acid-oxidation on TRRAP knockdown when compared to negative control transfected wells. q-PCR results were normalized to GAPDH, where control values were defined as 1 and changes in TRRAP transfected cells expressed as relative amounts compared with controls. (**b**) No difference in fatty acid (FA) oxidation was observed with ^{14}C-labeled [14]OA. The *p* values were calculated with Welch's test

decrease in the expression of APOC3 mRNA (−56%) upon knockdown of TRRAP with two different pools of siRNAs (Figure 5a). A decrease in secreted APOC3 protein was also seen on TRRAP knockdown both in the presence and absence of OA (−63%), when measured in the media by ELISA (Figure 5b). Because TRRAP knockdown reduced *C/EBPα* mRNA and protein, we measured hepatic APOC3 mRNA in liver-specific *C/EBPα* knockout mice and found a significant decrease in APOC3 expression (−40%; Figure 5c). We analyzed our RNA-seq database consisting of ~ 90 hiPSC lines and hiPSC-derived hepatocytes (HLCs)[31] and found a positive correlation (Pearson *r* = 0.6443, *p* < 0.001) between C/EBPα and APOC3 mRNA in HLCs, but not in undifferentiated hiPSCs (Pearson *r* = 0.06962, *p* = 0.25; Figure S4a). In silico analysis revealed a C/EBPα binding site in the promoter of *APOC3*, which is 100% conserved between humans and mice (Figure S4b). Thus, APOC3 is positively regulated by C/EBPα in hepatocytes, and TRRAP knockdown, by reducing C/EBPα, reduces APOC3 expression and secretion.

DISCUSSION

Unbiased cell-based screens together with high resolution microscopy to quantitate the lipid accumulation provides a powerful tool to investigate molecular targets and pathways involved with LD synthesis and growth.[12,13] In order to identify new genes involved in hepatic TG metabolism and potential new targets for NAFLD, we performed a siRNA-based high-content screen for LDs against human kinases and phosphatases. Among the novel positive hits was TRRAP, knockdown of which significantly decreased expression of DNL genes and de novo lipogenesis, in part by reducing C/EBPα expression. TRRAP knockdown also

reduced the expression and secretion of APOC3, a drug target for dyslipidemia and potentially NAFLD. Overall, this work provides proof of concept that a high-content screening assay for changes in LD phenotypes in hepatocytes is feasible and can identify new biology and potential therapeutic targets.

TRRAP, an adapter protein that has been identified as a member of various HAT multiprotein complexes including GCN5, Tip60, CBP/p300, and others.[32,33] TRRAP is required for p53/TP53-, E2F1-, and E2F4-mediated transcription activation.[32,34,35] A study in HepG2 cells reported decreased gene expression of *LXRα* target genes after shRNA-mediated knockdown of TRRAP.[36] Modulation of hepatic C/EBPα expression has a significant effect on DNL and hepatic lipid metabolism.[37,38] TRRAP has been shown to promote the acetylation of H3K9 and trimethylation of H3K4 at the promoters of a number of genes, including *LXRα*,[39–41] thus increasing their expression. We speculate that TRRAP increases C/EBPα and LXRα expression by promoting the acetylation of H3K9 at their promoters, and TRRAP knockdown therefore reduces expression of C/EBPα and LXRα, as well as genes regulated by them, including DNL genes,[42] SREBF1,[43] and APOC3 (Figure 5d). Further investigation exploring cell type specific roles of TRRAP in the liver and other metabolic tissues using conditional TRRAP knockout and overexpression in humanized models will be required to determine the specific molecular mechanisms by which TRRAP regulates hepatic lipid gene expression. Human genetic studies investigating effect of genetic variants in the *TRRAP* gene variants on liver fat and other metabolic phenotypes would be also be informative.

APOC3 is a validated therapeutic target for the treatment of hypertriglyceridemia.[44] An antisense oligonucleotide
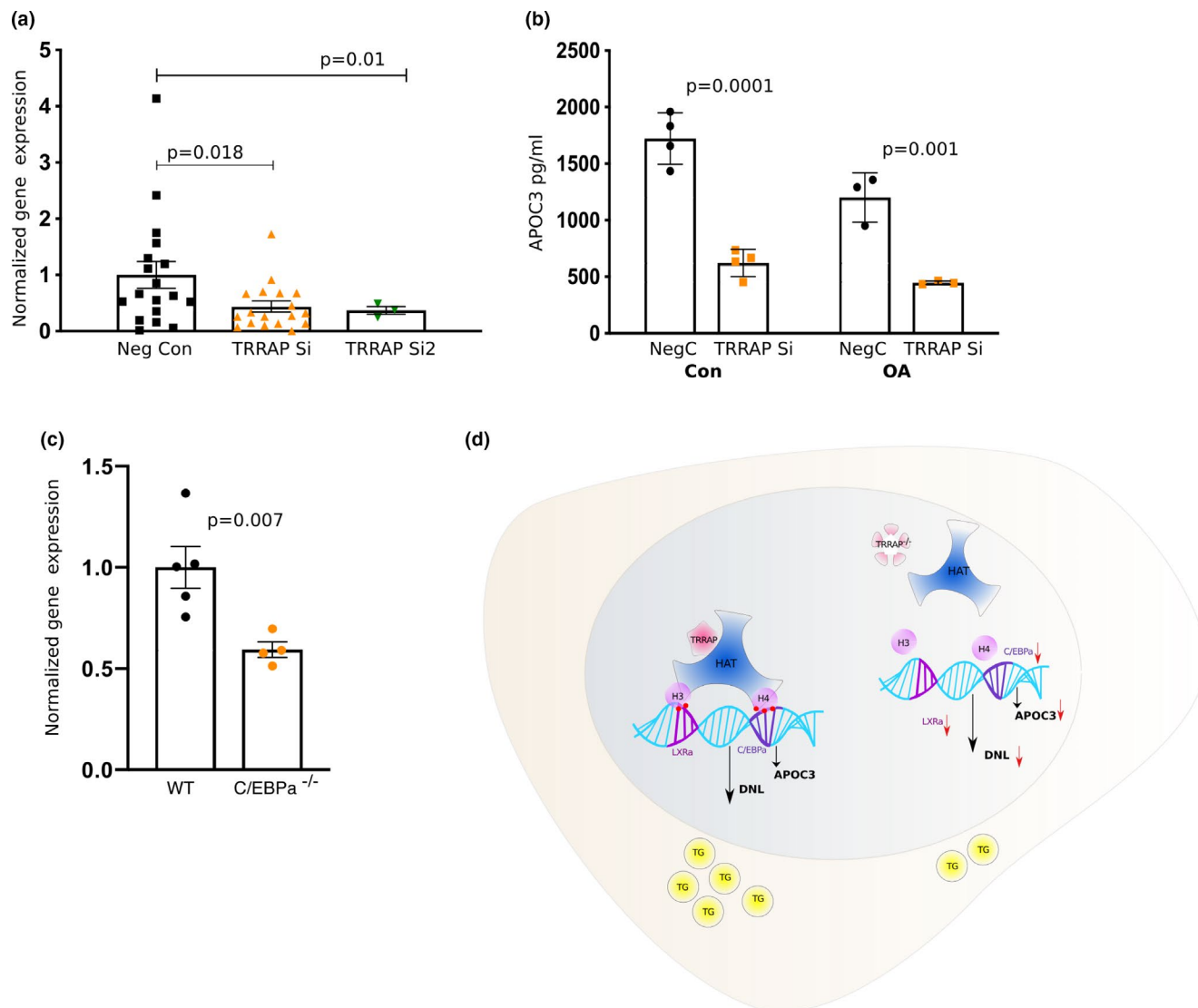
FIGURE 5 Knockdown of transformation/transcription domain-associated protein (TRRAP) reduces gene expression and secretory apolipoprotein C3 (APOC3). (**a**) Quantitative polymerase chain reaction (q-PCR) analysis showed decreased expression of *APOC3* and (**b**) Enzyme-linked immunosorbent assay (ELISA) showed decreased secretory APOC3 in the media of TRRAP siRNA compared with negative control transfected HuH-7 cells in the presence and absence of oleic acid (OA). (**c**) The q-PCR showed decreased expression of *APOC3* in liver specific C/EBPα knockout (KO) mice. (**d**) Schematic representation of the proposed role of TRRAP in regulating LXRα and C/EBPα-mediated triglyceride (TG) synthesis in hepatocytes. The q-PCR results were normalized to GAPDH, where control values were defined as 1 and changes in TRRAP transfected cells expressed as relative amounts compared with controls. ELISA was run with commercial standard using media alone as blank. All data represent the mean ± SEM. The *p* values were calculated with Welch's test

(ASO) to APOC3 is approved in Europe for the treatment of familial chylomicronemia[45] and a second generation galNAC-ASO to APOC3 is in clinical development.[46] Our data indicate that TRRAP silencing in HuH-7 cells reduces APOC3 expression and secretion, TRRAP has been reported to be a part of the PGC-1ß transcriptional complex,[47] and PGC-1ß regulates APOC3 gene expression,[47] suggesting the possible indirect regulation of APOC3.

This study establishes proof of concept for high content LD screening in HuH-7 cells for identification of genes that modulate hepatic steatosis. Our screen nominated TRRAP as a novel protein regulating hepatic LD accumulation and suggests that further study of TRAPP is warranted as a potential therapeutic target for NAFLD.

CONFLICT OF INTEREST
The authors declared no competing interests for this work.

AUTHOR CONTRIBUTIONS

REFERENCES

1. Brown DA. Lipid droplets: proteins floating on a pool of fat. *Curr Biol*. 2001;11:R446-449.
2. Martin S, Parton RG. Lipid droplets: a unified view of a dynamic organelle. *Nat Rev Mol Cell Biol*. 2006;7:373-378.
3. Walther TC, Farese RV Jr. Lipid droplets and cellular lipid metabolism. *Annu Rev Biochem*. 2012;81:687-714.
4. Koo S-H. Nonalcoholic fatty liver disease: molecular mechanisms for the hepatic steatosis. *Clin Mol Hepatol*. 2013;19:210-215.
5. Postic C, Girard J. Contribution of de novo fatty acid synthesis to hepatic steatosis and insulin resistance: lessons from genetically engineered mice. *J Clin Investig*. 2008;118:829-838.
6. Ginsberg HN. New perspectives on atherogenesis: role of abnormal triglyceride-rich lipoprotein metabolism. *Circulation*. 2002;106:2137-2142.
7. Nelson RH. Hyperlipidemia as a risk factor for cardiovascular disease. *Prim Care*. 2013;40:195-211.
8. Loomba R, Sanyal AJ. The global NAFLD epidemic. *Nat Rev Gastroenterol Hepatol*. 2013;10:686-690.
9. Friedman SL, Neuschwander-Tetri BA, Rinella M, Sanyal AJ. Mechanisms of NAFLD development and therapeutic strategies. *Nat Med*. 2018;24:908-922.
10. Echeverri CJ, Perrimon N. High-throughput RNAi screening in cultured cells: a user's guide. *Nat Rev Genet*. 2006;7:373-384.
11. Mattiazzi Usaj M, Styles EB, Verster AJ et al. High-content screening for quantitative cell biology. *Trends Cell Biol*. 2016;26:598-611.
12. Guo YI, Walther TC, Rao M, et al. Functional genomic screen reveals genes involved in lipid-droplet formation and utilization. *Nature*. 2008;453:657-661.
13. Whittaker R, Loy PA, Sisman E, et al. Identification of MicroRNAs that control lipid droplet formation and growth in hepatocytes via high-content screening. *J Biomol Screen*. 2010;15:798-805.
14. Daemen S, van Zandvoort MAMJ, Parekh SH, Hesselink MKC. Microscopy tools for the investigation of intracellular lipid storage and dynamics. *Molec Metabol*. 2016;5:153-163.
15. Bligh EG, Dyer WJ. A rapid method of total lipid extraction and purification. *Canadian J Biochem Physiol*. 1959;37:911-917.
16. Folch J, Lees M, Sloane Stanley GH. A simple method for the isolation and purification of total lipides from animal tissues. *J Biol Chem*. 1957;226:497-509.
17. Conlon DM, Thomas T, Fedotova T, et al. Inhibition of apolipoprotein B synthesis stimulates endoplasmic reticulum autophagy that prevents steatosis. *J Clin Invest*. 2016;126:3852-3867.
18. Fam TK, Klymchenko AS, Collot M. Recent advances in fluorescent probes for lipid droplets. *Materials (Basel, Switzerland)*. 2018;11:1768.
19. Liu Y, Millar JS, Cromley DA, et al. Knockdown of acyl-CoA:diacylglycerol acyltransferase 2 with antisense oligonucleotide reduces VLDL TG and ApoB secretion in mice. *Biochim Biophys Acta*. 2008;1781:97-104.
20. Murphy S, Martin S, Parton RG. Quantitative analysis of lipid droplet fusion: inefficient steady state fusion but rapid stimulation by chemical fusogens. *PLoS One*. 2010;5:e15030.
21. Breher-Esch S, Sahini N, Trincone A, Wallstab C, Borlak J. Genomics of lipid-laden human hepatocyte cultures enables drug target screening for the treatment of non-alcoholic fatty liver disease. *BMC Med. Genomics*. 2018;11:111.
22. Nunn ADG, Scopigno T, Pediconi N, et al. The histone deacetylase inhibiting drug Entinostat induces lipid accumulation in differentiated HepaRG cells. *Sci Rep*. 2016;6:28025.
23. Hopkins AL, Groom CR. The druggable genome. *Nat Rev Drug Discov*. 2002;1:727-730.
24. Handley MT, Mégarbané A, Meynert AM, et al. Loss of ALDH18A1 function is associated with a cellular lipid droplet phenotype suggesting a link between autosomal recessive cutis laxa type 3A and Warburg Micro syndrome. *Mol Genet Genomic Med*. 2014;2:319-325.
25. Chu R, Lin Y, Rao MS, Reddy JK. Cloning and identification of rat deoxyuridine triphosphatase as an inhibitor of peroxisome proliferator-activated receptor alpha. *J Biol Chem*. 1996;271:27670-27676.
26. Murr R, Vaissière T, Sawan C, Shukla V, Herceg Z. Orchestration of chromatin-based processes: mind the TRRAP. *Oncogene*. 2007;26:5358-5372.
27. Ramms B, Gordts P. Apolipoprotein C-III in triglyceride-rich lipoprotein metabolism. *Curr Opin Lipidol*. 2018;29:171-179.
28. Khetarpal SA, Zeng X, Millar JS, et al. A human APOC3 missense variant and monoclonal antibody accelerate apoC-III clearance and lower triglyceride-rich lipoprotein levels. *Nat Med*. 2017;23:1086.
29. Lee H-Y, Birkenfeld AL, Jornayvaz FR, et al. Apolipoprotein CIII overexpressing mice are predisposed to diet-induced hepatic steatosis and hepatic insulin resistance. *Hepatology*. 2011;54:1650-1660.
30. Samuel VT, Shulman GI. Nonalcoholic fatty liver disease as a nexus of metabolic and hepatic diseases. *Cell Metab*. 2018;27:22-41.
31. Pashos EE, Park YoSon, Wang X, et al. Large, diverse population cohorts of hiPSCs and derived hepatocyte-like cells reveal functional genetic variation at blood lipid-associated loci. *Cell Stem Cell*. 2017;20:558-570.e510.
32. Vassilev A, Yamauchi J, Kotani T, et al. The 400 kDa subunit of the PCAF histone acetylase complex belongs to the ATM superfamily. *Mol Cell*. 1998;2:869-875.
33. Ikura T, Ogryzko VV, Grigoriev M, et al. Involvement of the TIP60 histone acetylase complex in DNA repair and apoptosis. *Cell*. 2000;102:463-473.
34. Lang SE, McMahon SB, Cole MD, Hearing P. E2F transcriptional activation requires TRRAP and GCN5 cofactors. *J Biol Chem*. 2001;276:32627-32634.
35. Jethwa A, Słabicki M, Hüllein J, et al. TRRAP is essential for regulating the accumulation of mutant and wild-type p53 in lymphoma. *Blood*. 2018;131:2789-2802.
36. Unno A, Takada I, Takezawa S, et al. TRRAP as a hepatic coactivator of LXR and FXR function. *Biochem Biophys Res Comm*. 2005;327:933-938.
37. Qiao L, MacLean PS, You H, Schaack J, Shao J. knocking down liver ccaat/enhancer-binding protein alpha by adenovirus-transduced silent interfering ribonucleic acid improves hepatic gluconeogenesis and lipid homeostasis in db/db mice. *Endocrinology*. 2006;147:3060-3069.
38. Matsusue K, Gavrilova O, Lambert G, et al. Hepatic CCAAT/enhancer binding protein alpha mediates induction of lipogenesis and regulation of glucose homeostasis in leptin-deficient mice. *Mol Endocrinol*. 2004;18:2751-2764.
39. Tapias A, Zhou Z-W, Shi Y, et al. Trrap-dependent histone acetylation specifically regulates cell-cycle gene transcription to control neural progenitor fate decisions. *Cell Stem Cell*. 2014;14:632-643.

40. Wurdak H, Zhu S, Romero A, et al. An RNAi screen identifies TRRAP as a regulator of brain tumor-initiating cell differentiation. *Cell Stem Cell*. 2010;6:37-47.

41. van Straten EME, Bloks VW, Huijkman NCA, et al. The liver X-receptor gene promoter is hypermethylated in a mouse model of prenatal protein restriction. *Am J Physiol Regul Integr Comp Physiol*. 2010;298:R275-R282.

42. Bauer RC, Sasaki M, Cohen DM, et al. Tribbles-1 regulates hepatic lipogenesis through posttranscriptional regulation of C/EBPα. *J Clin Invest*. 2015;125:3809-3818.

43. Payne V, Au W-S, Lowe C, et al. C/EBP transcription factors regulate SREBP1c gene expression during adipogenesis. *Biochem J*. 2009;425:215-223.

44. Crosby J, Peloso GM, Auer PL, et al. Loss-of-function mutations in APOC3, triglycerides, and coronary disease. *N Engl J Med*. 2014;371:22-31.

45. Gaudet D, Brisson D, Tremblay K, et al. Targeting APOC3 in the familial chylomicronemia syndrome. *N Engl J Med*. 2014;371:2200-2206.

46. Alexander VJ, Xia S, Hurh E, et al. N-acetyl galactosamine-conjugated antisense drug to APOC3 mRNA, triglycerides and atherogenic lipoprotein levels. *Eur Heart J*. 2019;40:2785-2796.

47. Hernandez C, Molusky M, Li Y, Li S, Lin JD. Regulation of hepatic ApoC3 expression by PGC-1beta mediates hypolipidemic effect of nicotinic acid. *Cell Metab*. 2010;12:411-419.

SUPPORTING INFORMATION

Additional supporting information may be found online in the Supporting Information section.

How to cite this article: Abbey D, Conlon D, Rainville C, et al. Lipid droplet screen in human hepatocytes identifies TRRAP as a regulator of cellular triglyceride metabolism. *Clin Transl Sci*. 2021;14:1369–1379. https://doi.org/10.1111/cts.12988